The Results of the 2013 Pro-Am Wolf-Rayet Campaign

E. J. Aldoretta[1], N. St-Louis[1], N. D. Richardson[1], A. F. J. Moffat[1], T. Eversberg[2], G. M. Hill[3] and the World-Wide WR Pro-Am Campaign Team[4,5]

[1]*Université de Montréal, Canada*
[2]*Schnörringen Telescope Science Institute, Germany* [3]*W. M. Keck Observatory, United States* [4]*VdS Section Spectroscopy, Germany* [5]*Astronomical Ring for Access to Spectroscopy (ARAS), France*

Professional and amateur astronomers around the world contributed to a 4-month long campaign in 2013, mainly in spectroscopy but also in photometry, interferometry and polarimetry, to observe the first 3 Wolf-Rayet stars discovered: WR 134 (WN6b), WR 135 (WC8) and WR 137 (WC7pd+O9). Each of these stars are interesting in their own way, showing a variety of stellar wind structures. The spectroscopic data from this campaign were reduced and analyzed for WR 134 in order to better understand its behavior and long-term periodicity in the context of CIRs in the wind. We will be presenting the results of these spectroscopic data, which include the confirmation of the CIR variability and a time-coherency of ~ 40 days (half-life of ~ 20 days).

1 Motivation and Campaign Overview

Co-rotating interaction regions (CIRs) form in the winds of hot stars where fast material is colliding with slower material (or vise-versa) as the star rotates (Cranmer & Owocki 1996). This phenomenon was first discovered within the solar wind (Mullan 1984) and has since been seen in massive stars using several different observational methods. The exact cause of these structures could be attributed to phenomena at the base of the wind, such as magnetic fields or nonradial pulsations. While most O-type stars show DACs and NACs within their UV P Cygni lines, only a few WR stars have shown CIRs due to their saturated absorption components, some of which are WR 1, WR 6 and WR 134 (St-Louis (2013), Ignace et al. (2013) and Morel et al. (1999)). Using photometry, spectroscopy and polarimetry it is possible to learn more about these features and how they are formed.

Morel et al. (1999) studied the strong spectral variations of WR 134. An intensive campaign of spectroscopic and photometric monitoring of this star took place in order to reveal the nature of these variations. A coherent 2.25 ± 0.05 day periodicity in changes of the He II $\lambda 4686$ emission line was confirmed. The global pattern of variability, however, changed with each epoch. While this period was strongly detected within the spectroscopic data, it was only marginally detected in the photometric data. In an attempt to better understand this period found in the spectroscopic data, we organized a collaboration between amateur and professional astronomers.

During the summer of 2013, a 4-month Wolf-Rayet (WR) campaign began on WR 134, WR 135 and WR 137. Each of these targets were chosen in order to observe different features: WR 134 is known to show co-rotating interaction regions (CIRs) in the spectral lines (Morel et al. 1999), WR 135 is known to show large clumpy structures in its wind (Lepine et al. 1996) and WR 137 is a long-period WR+O binary system with possible CIRs (Lefèvre et al. 2005). All three of these stars could benefit from long-term observations and are relatively easy for amateurs to observe due to their visual magnitudes ($V \sim 8.1$, $V \sim 8.1$ and $V \sim 7.9$, respectively). Several types of data were collected, including interferometry from the CHARA Array, photometry, broad-band polarimetry and spectroscopy. A total of 10 sources have contributed to the spectroscopic data of the campaign, the majority of which was collected on the island of Tenerife. For the object WR 134, the spectroscopic data have been analyzed and the results are presented.

Tab. 1: List of spectroscopic data sources, along with corresponding resolving powers and wavelength coverages.

Observatory	$R(\lambda/\Delta\lambda)$	λ coverage (Å)
Professional Facilities		
Teide	10,000	4500 - 7400
Keck	13,000	4000 - 10000
OMM	4,000	4700 - 6000
DAO	5,500	5100 - 6000
Ondřejov	10,500	5200 - 5750
NOT	11,800	3500 - 6800
Amateur Contributors		
Potter	7,500	5300 - 5850
Li	5,300	5250 - 5600
Strachan	5,300	5300 - 5700
Leadbeater	5,350	5200 - 5600

The spectrosocpic data collected for this project

were taken with a large group of astronomers from 25 May 2013 to 06 October 2013. Ten different observatories contributed to the spectroscopic data for these WR stars, five of which are professional facilities (outlined in Table 1). All observers participating in the campaign observed at least the He II $\lambda5411$ emission line, where the CIR perturbations can be easily detected due to the strength of line along with its relative isolation. All data were reduced using standard techniques.

2 Data Analysis

Several calculations were made in order to determine if the 2.25-day period that was found by Morel et al. (1999) would be present within these spectroscopic data. Our first method was to first create an average spectrum in velocity space. Then, a Scargle (1982) periodogram was created over each velocity. Figure 1 shows the results of these calculations. It can be seen that the frequency ~ 0.443 ($P = 2.25$ days) is strong over the majority of the He II $\lambda5411$ emission line. The first harmonic of this frequency ($2f$), along with both of their one-day sampling aliases (1 - f and 1 - $2f$) are also detected

where I_j is the intensity of the line and λ_j is the wavelength. Two dimensionless quantities can be calculated from these moments: the skewness by $\mu_3/\mu_2^{3/2}$ and the kurtosis by μ_4/μ_2^2. A time-dependent Scargle analysis was then conducted on these moments, resulting in a mean period of $\sim 2.255 \pm 0.007$ days.

Once this period was calculated and confirmed, phased difference images from the mean were created in five-day (≈ 2 cycles) segments with a total of 23 images for the entire run. An arbitrary image was chosen from these from which a normalized 2-D cross-correlation was made from the images before and after the fixed image. This was repeated with two other images based on their good time-coverage of data, all showing similar results. The cross-correlations were calculated by:

$$Xc_{ij} = \frac{\Sigma_{jk} I_{1jk} \times I_{ijk}}{\Sigma_{jk} I_{1jk}^2}, \qquad (2)$$

with $i = 1$ being the fixed image and j and k referencing the location of the pixels. Then a Gaussian function plus constant background was arbitrarily fit to every data point of the cross-correlation, with the peak coinciding with the maximum correlation. The artificial correlation of 1.0 of the image with itself was ignored.
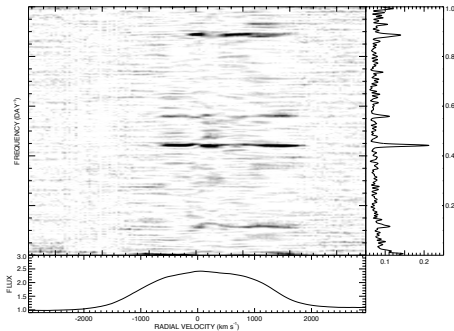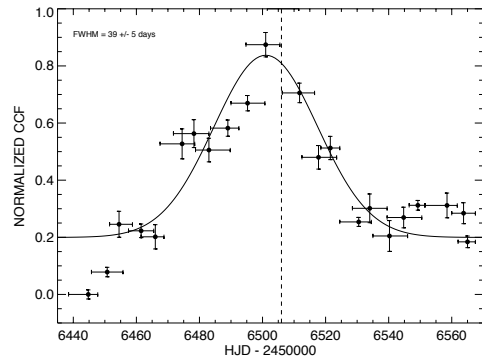

Fig. 1: 2-D Scargle periodogram (Scargle 1982) for the velocity space around the He II $\lambda5411$ line. The bottom panel shows the average spectrum of the entire data set. The right panel shows the Scargle periodogram. The middle panel shows the grey-scale of the Scargle analysis for each velocity. It can be seen that the frequency of ~ 0.0443 d^{-1} is the strongest peak.

Moments of the He II line were also calculated over the entire data set. The central n^{th} moment is given by:

$$\mu_n = \Sigma_j(\lambda_j - \bar{\lambda})^n I_j/\Sigma_j I_j$$
$$\bar{\lambda} = \Sigma_j \lambda_j I_j/\Sigma_j I_j, \qquad (1)$$

Fig. 2: Cross-correlation of phased gray-scale difference images. Time frame for each image is displayed as x-axis error bars. The reference image is shown along dotted line and was ignored for the Gaussian fit.

Figure 2 shows the time-coherency for the CIR of ~ 40 days (18 cycles) that was found. This was determined by fitting a Gaussian to both (a) the entire data set and (b) both sets of non-overlapping data points in time and calculating the mean FWHM of the three results. This 40-day time-coherency was also present in a time-dependent Scargle periodogram created for the skewness and kurtosis of
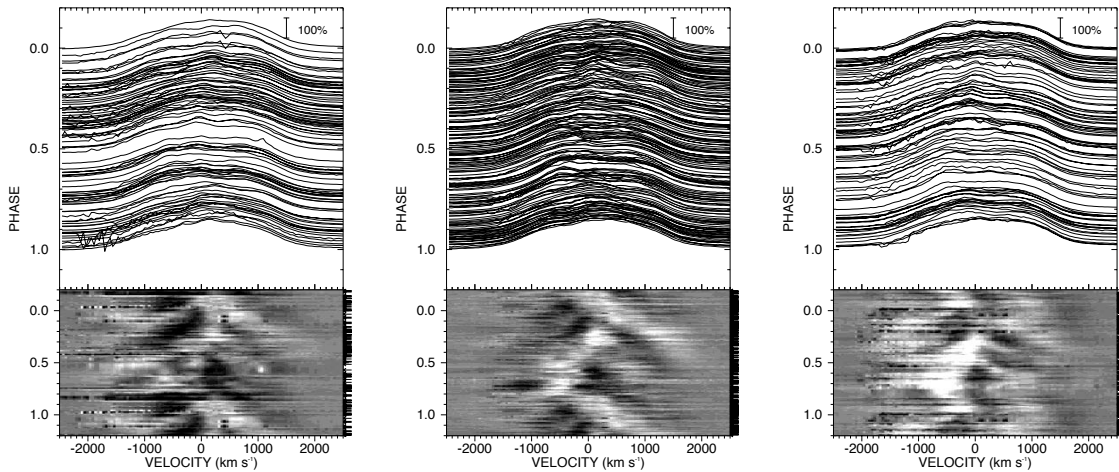
Fig. 3: : Difference gray-scale images of the spectra are shown. The images are increasing with time from left to right and are grouped in 40-day (18 cycle) segments.

this line as well. Between HJD-2456467 and HJD-2456517, the 2.255-day period is the strongest in both of these moments, which corresponds with the time-coherency found in the cross-correlation. This cross-correlation also shows that this CIR displays a half-life time (or decay time) equivalent to the HWHM of the Gaussian, or ~ 20 days.

Once the time-coherency was determined for WR 134, new difference images were created in order to see how the CIRs change every 40 days (see Figure 3). These images show the main CIR rotating within the wind, but also shows weaker CIRs with other separation angles relative to the rotating star underneath. Dessart & Chesneau (2002) created models of CIRs in WR star winds, which showed a similar brightness pattern consistent with multiple CIRs.

3 Summary and Future Work

We were able to determine a CIR period of 2.255 ± 0.007 days, which agrees with the results by Morel et al. (1999). Once the period was determined, the spectra were then organized by phase in order to create difference grey-scale plots for 5-cycle segments. These grey-scale plots were cross-correlated with each other, showing either a coherence timescale of $\sim$

40 days (18 cycles) or a half-life time of ~ 20 days for the CIRs. Gray-scale difference plots for 40-day segments were created and show how the CIR changes with the coherence timescale. When compared to the model by Dessart & Chesneau (2002) it can be determined that more than one CIR is likely present in the wind. Future modeling and kinematics could reveal information on the physics causing large-scale structures in WR winds.

References

Cranmer, S. R. & Owocki, S. P. 1996, ApJ, 462, 469

Dessart, L. & Chesneau, O. 2002, A&A, 395, 209

Ignace, R., Gayley, K. G., Hamann, W.-R., et al. 2013, ApJ, 775, 29

Lefèvre, L., Marchenko, S. V., Lépine, S., et al. 2005, MNRAS, 360, 141

Lepine, S., Moffat, A. F. J., & Henriksen, R. N. 1996, ApJ, 466, 392

Morel, T., Marchenko, S. V., Eenens, P. R. J., et al. 1999, ApJ, 518, 428

Mullan, D. J. 1984, ApJ, 283, 303

Scargle, J. D. 1982, ApJ, 263, 835

St-Louis, N. 2013, ApJ, 777, 9

Michael Corcoran: Do new CIRs re-appear at the same phase after each 40-day CIR cycle?

Emily Aldoretta: No, we do not see the same configuration of CIRs re-appear because we do not see the correlation function more than once within our data set, possibly in part due to the finite length of the data stream.

John Eldridge: Could the signal of multiple CIRs actually be because the star is precessing/wobbling as it rotates?

Emily Aldoretta: Possibly, but not on a timescale shorter than our observations. We should perhaps watch for signs of this in the future.

Andy Pollock: Could you tell more about the long-term coherence of the 2.25-day and 40-day periods?

Emily Aldoretta: According to the cross-correlation analysis, the 2.25-day period is seen to be relatively coherent for 40 days for any given reference point in time. Other than the 2.25-day period, there is no evidence for another period in our data.

Peredur Williams: Is the 2.25-day period variation coherent, as if the CIRs originated on the same points on the star?

Emily Aldoretta: This is an interesting point, and our best guess is that we see multiple CIRs coming and going on various time scales on a stellar rotation period of 2.25 days. Whether each CIR originates at the same rotating point on the star remains to be demonstrated.

Thomas Eversberg: Repeating CIR features after 18 cycles smells like a resonance effect. That would be in conflict to the idea of hot spots as the origin of CIRs. What is your impression about that?

Emily Aldoretta: The 18-cycle time-coherency does not represent a periodic repetition, but a time-coherency for which the cross-correlation function fades away.